The role of mineral aerosols in shaping the regional climate of West Africa

Marc P. Marcella[1] and Elfatih A. B. Eltahir[1]

Received 21 December 2012; revised 3 November 2013; accepted 3 November 2013.

[1] This article examines the role of mineral aerosols in the regional climate of West Africa. Analysis is completed by comparing two 30 year simulations using a regional climate model (RegCM3-IBIS). The two simulations are identical in structure except one includes the representation of mineral aerosols via a fully coupled radiatively interactive dust emissions and aerosol tracer model; the other simulation does not. To discern the impact of dust on West Africa's climate, comparisons are made between the two simulations' surface climatology as well as atmospheric dynamics. It is found that RegCM3-IBIS and its dust model perform well in simulating the temporal and spatial distributions of mineral aerosols over the Sahel and Sahara. Consistent with previous studies over the region, RegCM3-IBIS simulates high-dust loading over the region (aerosol optical depth of 0.5–1.1), which results in significant incident shortwave radiation attenuation (25–50 W/m^2) and temperature cooling (0.5°C–1.25°C). Depending on the underlying surface brightness, the top of atmosphere net radiative forcing may be positive (bright desert surfaces) or negative (dark, vegetated surface) with important implications on surface temperature cooling. Here it is proposed that the effects of dust on West African rainfall are distinctly different across the ocean-land border and the desert border region of the Sahel/Sahara. Nevertheless, in both regions, the change in rainfall is less than 10% of the total annual values. Therefore, this work concludes that the current, observed, dust loading over West Africa does not significantly affect rainfall via changes in the radiation budget. However, it is important to note that this work does not include mineral aerosol effects on sea surface temperatures, which may be significant in influencing the results.

Citation: Marcella, M. P., and E. A. B. Eltahir (2014), The role of mineral aerosols in shaping the regional climate of West Africa, *J. Geophys. Res. Atmos.*, *119*, doi:10.1002/2012JD019394.

1. Introduction

[2] Mineral aerosols are known to have important implications in shaping the global climate via effects on radiation, temperature, and precipitation [*Tegen et al.*, 1996; *Sokolik et al.*, 2001]. However, alternatively, atmospheric processes such as rainfall and wind are also known to affect dust emissions. For example, *Brooks and Legrand* [2000] use an infrared difference dust index based on atmospheric brightness temperatures to conclude that spatial and temporal patterns of North African dust production decrease in spring and summertime due to the passage of convective disturbances across the Sahel during that time period. They found further evidence that wet season rainfall totals have an impact on dust production in the latter part of the following dry season. Similarly, the Saharan Dust Experiment of 2000 suggested that Saharan dust aerosol exerts the largest local and global direct radiative effect of all aerosol species and should be considered explicitly in global radiation budget studies [*Haywood et al.*, 2003]. Likewise, the African Monsoon Multidisciplinary Analyses (AMMA) project included a special observing field campaign to focus on aerosol and radiation processes in January and February of 2006 [*Haywood et al.*, 2008]. In these observations, they find that while biomass aerosols are significantly absorbing of radiation, mineral dust aerosols are less absorbing and more scattering. The research concludes that the influence of both mineral dust and biomass burning on the radiation budget is significant throughout the observing period, implying that meteorological models should include their radiative effects for accurate forecasts and climate simulations.

[3] To this point, many studies have examined the mineral aerosol effect on climate via general circulation models (GCMs) [*Miller and Tegen*, 1998; *Mahowald et al.*, 1999; *Woodward*, 2001; *Lau et al.*, 2009]. Focusing over West Africa, *Yoshioka et al.* [2007] used a GCM coupled to a slab ocean model to simulate reduced precipitation over the Intertropical Convergence Zone (ITCZ) including the

[1]Department of Civil and Environmental Engineering, Massachusetts Institute of Technology, Cambridge, Massachusetts, USA.

Corresponding author: M. P. Marcella, Parsons Laboratory for Environmental Science and Engineering, Massachusetts Institute of Technology, MIT-Building 48-216, Cambridge, MA 02139, USA. (marcpace@mit.edu)

2169-897X/14/10.1002/2012JD019394

Table 1. Comparative Table Listing the Simulation Design and Key Findings of Both *Konare et al.* [2008] and *Solmon et al.* [2008] as Well as the Results of our DCONT-CONT Simulations[a]

	Konare et al. [2008]	*Solmon et al.* [2008]	DCONT-CONT
Model	RegCM3-BATS	RegCM3-BATS	RegCM3-IBIS
ICBCs	NCEP-NNRP2	NCEP-NNRP2	ECMWF-ERA-40
Time period	1969–2006	1996–2006	1972–2002
Resolution	60 km	60 km	30 km
AOD range	0.5–1.0+	0.4–1.0	0.5–1.1
ΔSurface Temperature	–0.5°C to –2°C	Not Shown	–0.5°C to –1.25°C
ΔSurface SW Radiation	0 to –90 W/m^2	0 to –50 W/m^2	0 to –50 W/m^2
ΔRainfall	–0.5 to –1.5 mm/d	–1.0 to +0.75 m/d	–0.2 to +.5 m/d

[a]Values are taken either from the text or from the averaged over the Sahel/Sahara from figures published in both studies.

Sahel region and increased precipitation south of the ITCZ when the dust radiative forcing is included. However, in observed sea surface temperature (SST)-forced simulations, negative precipitation changes are restricted only over North Africa. These changes are considered to be due to the cooling of global tropical oceans as well as the cooling of the troposphere over North Africa in response to the dust radiative forcing.

[4] Yet the influence dust has on local weather and climate has only recently been examined in the regional modeling literature. For example, on the forecasting side, including a representation of mineral aerosols in a numerical weather prediction model significantly improved the simulation of radiative fluxes, surface temperatures, and thermodynamic structure over West Africa [*Milton et al.*, 2008]. While on the climate scale, the work of *Zhang et al.* [2009] used a regional climate model coupled to a dust model to examine regional feedbacks over East Asia; their results found a near 1°C cooling across dust sources in China. Likewise, *Konare et al.* [2008] examined the shortwave radiative forcing of Saharan dust on the West African Monsoon using RegCM3-BATS. Their results indicated a decrease in rainfall on the order of 0.5–1.5 mm/d across some portions of the Sahel with surface cooling on the order of 1°C–2°C across the heavy dust loaded regions. With some regions in their simulations reaching an aerosol optical depth (AOD) value of well over 1.0, the surface shortwave incident radiation is attenuated by more than 90 W/m^2 over these locations. As a result, the authors conclude that the surface cooling across the Sahara decreases the meridional gradient of moist static energy and results in a weakening of the monsoon energy pump. A further study completed by *Solmon et al.* [2008] investigates the dust aerosol impact on regional precipitation over West Africa and the sensitivity to absorption properties. In this work, a 10 year simulation found only a slight decrease in rainfall (0.4 mm/day) over the Sahel with an actual slight increase across the northern Sahel and southern Sahara region. The contrasting findings may be due to a dust loading which is significantly smaller than *Konare et al.* [2008] with AOD values varying from 0.4 to 0.8 across the Sahara in *Solmon et al.* [2008]. As a result, surface shortwave radiation attenuation (30–50 W/m^2) is significantly smaller in *Solmon et al.* [2008]. Another important finding in this work is the sensitivity of mineral aerosol parameters to the effects that dust has on the regional climate. *Solmon et al.* find that the single scattering albedo (SSA) and its magnitude largely determine the intensity of precipitation decrease versus increase as well as the latitudinal limit between these two responses. In any event, these studies did not examine the effects of dust on the surface heat fluxes or the diurnal cycle. That is, both studies examined mean summertime changes in temperature, radiation, and rainfall. Here the aim is to provide a detailed analysis of the dust-climate feedback that investigates the physical processes or mechanisms that shape the role of mineral aerosols in the climate of West Africa. Nevertheless, Table 1 provides a comparison of the simulation design of those two studies and their key findings compared to the results found in this work.

2. Experimental Design

[5] Two 30 year simulations of RegCM3-IBIS, centered at 14°N and 3°E at 30 km resolution, with 180 points in the zonal and 200 points in the meridional direction using a Mercator projection are performed to evaluate the effects of mineral aerosols on the climate of West Africa. The first year of simulation is used as model spin-up and therefore not used in analysis. The domain covers most of West Africa from the Mediterranean Sea in the north to the Congo and Atlantic Ocean in the south. Figure 1 represents the model domain as well as topography and vegetation biomes. The prescribed vegetation biomes are taken from the potential natural vegetation data set of *Foley et al.* [1996] with cropland added from the work of *Ramankutty and Foley* [1998]. The Grell scheme is chosen to model moist convection within RegCM3-IBIS with the Fritsch and Chappell closure employed [*Grell et al.*, 1994]. All other physics packages used in these simulations are of the standard configuration of RegCM3-IBIS; the authors refer readers to *Pal et al.* [2007] and *Winter et al.* [2009] for a more detailed model description.

[6] Seasonal analysis of surface and atmospheric fluxes are performed on a zonally averaged (10°W–10°E) box from 6°N–25°N also shown in Figure 1. Initial and boundary conditions are implemented from the ERA-40 reanalysis data set for the period of 1972–2002 [*Uppala et al.*, 2005]. Lateral boundary conditions were forced by applying the sponge relaxation of *Perkey and Kreitzberg* [1976]. SSTs are prescribed to RegCM3 from the Hadley Centre Met Office's Global Ice and Sea Surface Temperature optimally interpolated data set [*Rayner et al.*, 2006]. The SST data sets are $1^\circ \times 1^\circ$ monthly resolution and are based on in situ and

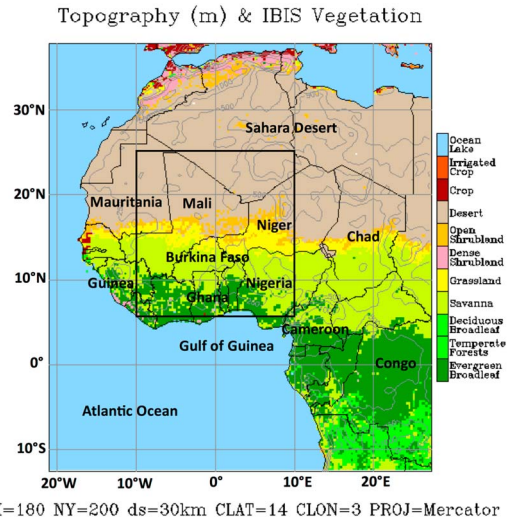

Figure 1. Domain implemented for RegCM3-IBIS simulations. Vegetation biomes are shaded and topography (in meters) contoured. Boxed region shows area where spatial averages are computed for (10°W–10°E, 6°N–25°N).

satellite observations. This simulation will be hereafter referred to as CONT. Another identical 30 year simulation with RegCM3-IBIS but also coupled to the dust emission scheme of *Zakey et al.* [2006] and the aerosol tracer model of *Solmon et al.* [2006] is completed over West Africa, hereafter referred to as DCONT.

3. Mineral Aerosol Model Performance

[7] While the dust model of RegCM3 has already been rigorously compared to extensive ground and satellite observations over West Africa with simulated results comparing favorably to observations [e.g., *Zakey et al.*, 2006; *Konare et al.*, 2008], here an additional comparison is made to a newer satellite product, NASA's Multiangle Imaging Spectroradiometer (MISR). Aboard the Terra satellite, MISR contains nine cameras that observe the Earth at different viewing angles. In this study, MISR Level 3 Component Global Aerosol Product, at $0.5° \times 0.5°$ resolution, is used for AOD values at 555 nm. The temporal coverage used in this analysis is from 2001 to 2010. It has been shown that the MISR retrieval algorithm performs well over bright desert surfaces [*Abdou et al.*, 2005; *Marcella and Eltahir*, 2010]. For further information on the MISR data set, the authors refer the reader to *Martonchik et al.* [1998].

[8] Figure 2 displays the zonally averaged seasonality of aerosol optical depth (AOD) or aerosol suspension over West Africa in satellite observations and the DCONT simulation. As seen in the figure, RegCM3-IBIS does well in capturing the seasonality of AOD across the Sahara and Sahel. Namely, the model successfully simulates a daily AOD maxima during the summer months of June, July, August (JJA) from 15°N to 20°N of 0.5–0.7. Likewise, RegCM3-IBIS properly reproduces the south-north gradient of aerosol suspension as seen in MISR observations, reflecting the monsoon and rainy season in the south, the dry "dust belt" of the Sahel and Sahara, and the less dusty region of North Africa. However, noticeable in Figure 2 is the large underestimation of RegCM3's modeled AOD in December, January, February, March (DJFM) from the coastline to 12°N. It is important to note that over this region during this time of the year, extensive biomass burning occurs due to cropland clearing and dry lightning strikes [*Liousse et al.*, 1996; *Cooke et al.*, 1999; *Junker and Liousse*, 2008]. While these organic carbon aerosols are apparent in AOD observations, only mineral aerosols are included in the DCONT simulation; thus, it is to be expected that the model would show a bias over the Gulf of Guinea during the winter months.

[9] DCONT's spatial performance in modeled summertime June, July, August, September (JJAS) dust suspension is examined in Figure 3. RegCM3's dust emission and aerosol tracer model accurately captures the summer dust "hot spots" of the Bodele Depression, Niger, Mali, and Mauritania as seen in MISR observations and described in *Prospero et al.* [2002]. These results are similar to the work of *Konare et al.* [2008] who also find that RegCM3 adequately reproduces the mineral aerosol climatology of the region and the dust belt of the Sahel-Sahara region [*Prospero et al.*, 2002]. However, these results are slightly less than *Konare et al.* [2008] which see average JJA AOD values well over 1.0 across the entire region but match very closely to *Solmon et al.* [2008] estimates of AOD values ranging from 0.4 to 0.8. Nevertheless, overestimations do appear in the dust loading regions of north Niger and Mauritania as seen in Figure 3. This bias may be a result of MISR sampling error as the satellite has known issues in retrieving AOD values in the lowest 1 km of the atmosphere over heavy dust loading regions [*Konare et al.*, 2008]. In contrast, the model underestimates AOD across the north and at the boundaries. This is most likely a result of imposing zero boundary conditions which may lead to excessive diffusion out of the domain [*Marcella and Eltahir*, 2010].

[10] Unlike boreal summer, winter months signal a southern shift in the maxima of aerosol suspension as biomass burning becomes prevalent along the Gulf of Guinea coastline (see Figure 2). As mentioned prior, only mineral aerosols are represented in DCONT; therefore, the model does not capture this spatial signature. However, RegCM3 is able to reproduce the more southern progression of dust suspension across southern Chad, northern Nigeria, and Burkina Faso (not shown). With the recession of the monsoon, these regions experience some dust events.

[11] Another important parameter in accurately modeling a region's aerosol climatology is the single scattering albedo (SSA). The parameter quantifies the ratio of the amount of light scattered to the total light extinction caused by an aerosol. It is important to note that the SSA is determined via the composition as well as the physical size of the particulate and is wavelength dependent. Given similar compositions, a higher value of SSA would signify aerosols that scatter more than absorb shortwave radiation (a large SSA) and therefore of small particle size. In RegCM3-IBIS, the largest values of SSA occur over regions where there is significant dust loading such as Mali, Niger, and Chad. JJA values of this region (0.9–0.95) match very well with the satellite observations of *Kaufman et al.* [2001] and *Hsu et al.* [2004] and the modeling work of *Konare et al.* [2008] and *Solmon et al.* [2008] yet smaller than the single scattering values of 0.99

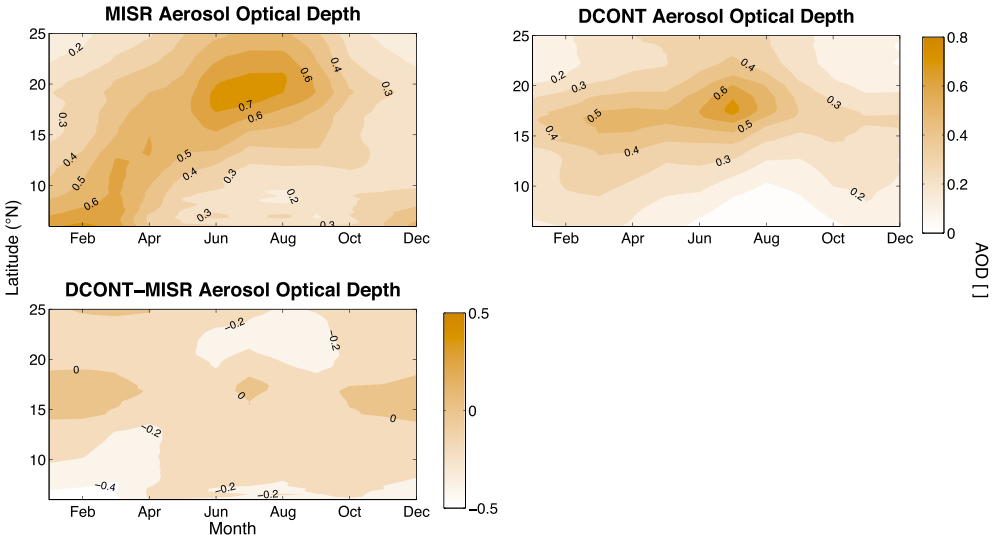

Figure 2. Zonally averaged (10°W–10°E) monthly averaged aerosol optical depth (AOD) in MISR observations and DCONT simulation from 6°N to 25°N. Also shown is model bias with MISR.

from the AMMA field campaign [*Haywood et al.*, 2008]. The implications on the energy balance over the region will be discussed in further detail below.

[12] Examining the mean JJA vertical profile of dust concentration (in the meridional and zonal directions) reveals that mineral aerosols extend vertically to about 500 mb, implying that not only are the vertical transport by convection and a deep boundary layer important but also suggesting that effects of dust may not just occur in the surface climatology (Figure 4). As expected, the largest concentrations aloft occur where dust loading at the surface is the greatest—at 10°W and 10°E between 15°N and 20°N. Also noticeable is the effect of atmospheric dynamics such as the African Easterly Jet (AEJ) on the distribution of dust aloft. For example, mineral aerosols are transported south as seen in the latitudinal cross section caused by the northerly Harmattan winds. Likewise, the effect of the AEJ on mineral aerosol distribution in the zonal is clearly seen as dust concentrations aloft are spread westward from 20°E to 20°W. More specifically, the Saharan Air Layer (SAL) around 650 mb is clearly evident in the longitude cross section of dust concentration. The SAL is characterized as a warm dusty layer

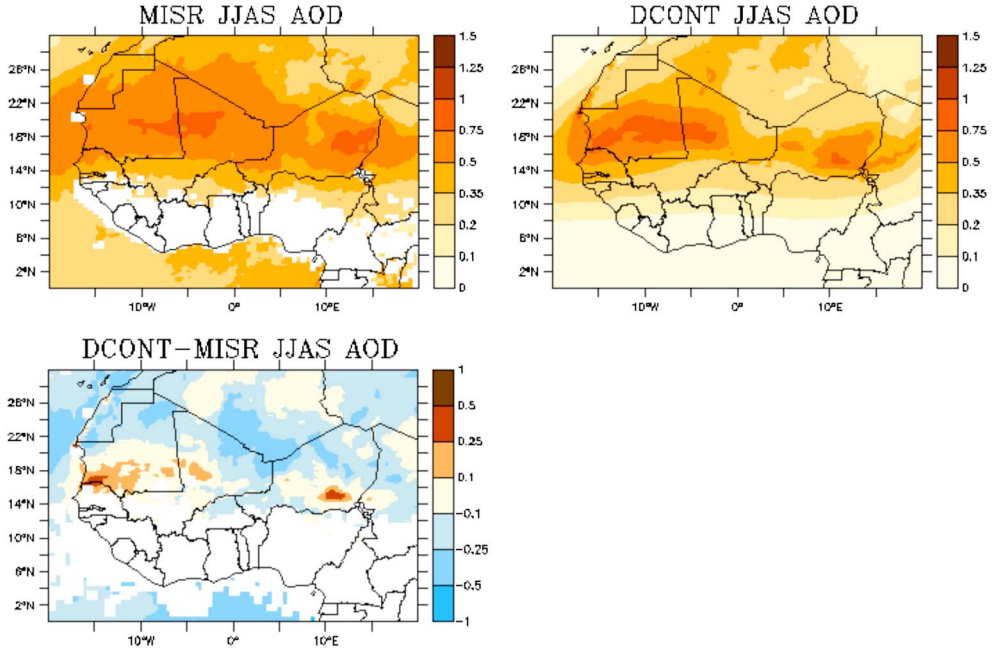

Figure 3. Average JJAS daily AOD for MISR observations and DCONT simulation. Also plotted is model bias (DCONT-MISR) for simulated AOD.

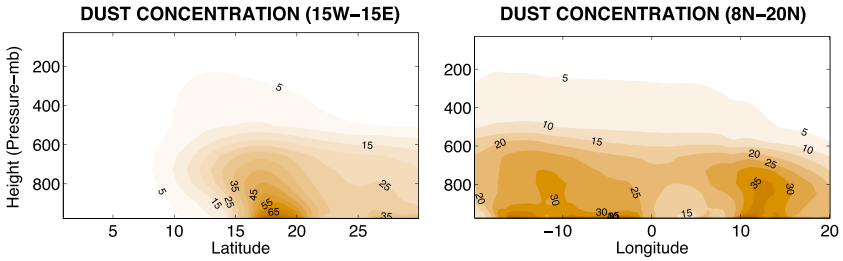

Figure 4. Vertical cross sections of JJA averaged dust concentration (μg/kg) presented in both the latitude (S-N) averaged between 15W-15E and longitude (W-E), averged between (8N-20N).

aloft around 600–700 mb that is known to transport dust across the Atlantic Ocean and critical in the formation of Atlantic hurricanes [*Carlson and Prospero*, 1972]. RegCM3 does well in simulating this midlevel feature, indicating that the model adequately represents the vertical distribution of dust over West Africa. These results are similar to those of *Konare et al.* [2008] which find vertical penetration of dust up to 500 mb.

4. Seasonal Surface Climatology

4.1. Radiation Effects

[13] As discussed prior, mineral aerosols both scatter and absorb shortwave energy aloft. Over Niger, Chad, and Mali, it is found that smaller dust particles are significantly more prevalent than larger particulates (large SSA values). Figure 5 quantifies the effect of dust suspension on the JJAS mean clear sky net surface shortwave and top of atmosphere (TOA) radiation. Clearly visible in the figure is the large impact at the surface across the entire Sahara and Sahel region. A background surface radiative forcing of –5 to –10 w/m^2 occurs across all of West Africa with a radiative forcing of –20 to –40 W/m^2 across the Sahara and Sahel dust belt with the highest values closest to the dust source regions of Chad, Niger, Mali, and Mauritania. The surface shortwave reduction is indicative of surface cooling. Moreover, as expected, the radiative forcing at the surface follows the spatial distribution of AOD with the magnitude following the estimates of *Liao and Seinfeld* [1998] which range from –30 to –40 W/m^2 per unit AOD. Likewise, these results lie within other modeled results of *Konare et al.* [2008] and *Solmon et al.* [2008] (see Table 1).

[14] Conversely, the TOA net shortwave radiative forcing is significantly smaller than that at the surface with maximum radiative forcing of –10 W/m^2. Due to the high-surface albedo over the Sahara and the large scattering caused by dust over this region (SSA values), it is expected that the TOA radiative forcing would be small over the desert region. In fact, nearly no TOA radiative forcing occurs over the Sahara. In contrast, the darker albedos of the Sahel and the Atlantic Ocean result in a larger negative TOA radiative forcing (5–10 W/m^2 over the Sahel and 10–15 W/m^2 over the Atlantic Ocean). Nevertheless, all these results are similar to the findings of other Regional Climate Model (RCM) aerosol studies over this region [e.g., *Miller et al.*, 2004; *Zakey et al.*, 2006; *Yoshioka et al.*, 2007]. It is important to note that the difference between the TOA and surface shortwave radiation is indicative of the absorbed shortwave throughout the column. As can be seen, there is some significant absorption which is proportional to the diabatic heating rate in the column. As will be shown, there is only slight warming aloft as a result. This term is small compared to the effect of the TOA negative forcing, which is consistent with the high SSA values of dust in the shortwave spectrum [*Konare et al.*, 2008].

4.2. Two Meter Temperature

[15] With a reduction of shortwave incident radiation on the order of 20–40 W/m^2, a mean surface cooling of 1°C occurs throughout the Sahara Desert (see Figure 6). As expected, maximum cooling occurs in the regions of maximum dust loading (highest AOD values) where average JJA temperatures cool by more than 1.25°C (see Figure 6). As winter approaches, a southern shift occurs in the maximum

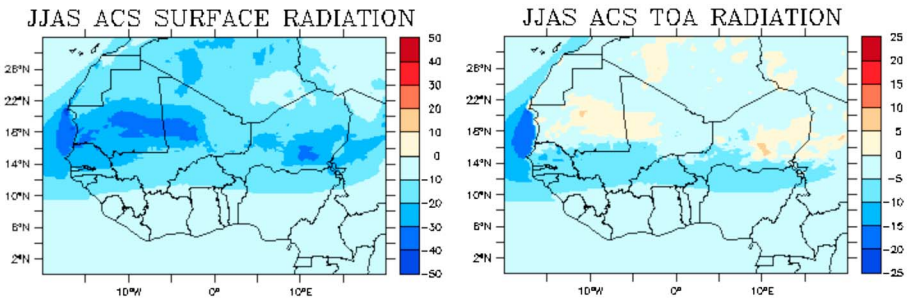

Figure 5. Same as Figure 3 but for DCONT's clear sky (cloud effects removed) surface net shortwave radiation and top of atmosphere (TOA) net shortwave radiation both in (W/m^2).

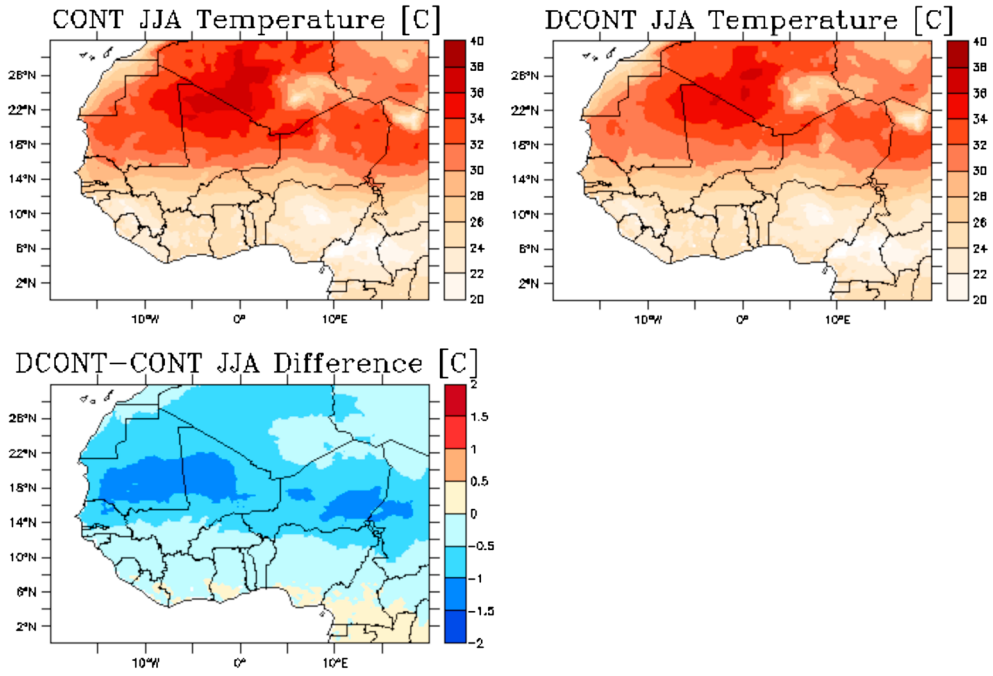

Figure 6. Average JJA daily 2 m temperature (°C) for CONT and DCONT simulations. Also plotted is difference due to dust emissions (DCONT-CONT).

cooling as the dust burden increases across Nigeria, Burkina Faso, and southern Mali (not shown). Given this region is more vegetated and hence has a darker surface albedo, the dust radiative forcing at the surface and at the TOA are both negative and are at very similar magnitudes, resulting in sizable net reduction in temperature that is also similar in magnitude both at the surface and TOA (see Figures 9 and 10). Likewise, ignoring the effects of longwave radiative effects of dust may also change the heating signal or change in vertical temperature profile (via increased longwave emissions) as alluded to in a similar finding and study of *Konare et al.* [2008]. However, the effects of dust on the longwave radiation have been shown to be of much less importance and smaller in magnitude as shown in the work of *Solmon et al.* [2008]

4.3. Annual Rainfall

[16] Figure 7 displays the average annual rainfall in both CONT and DCONT as well as the differences between the two simulations. As seen in the figure, little change in magnitude or spatial distribution results from including dust emissions; the well documented tight gradient in rainfall from the Guinean coastline to the Saharan desert is still apparent. However, a slight decrease in rainfall does occur across the Gulf of Guinea coastline (50–250 mm/yr), but it is less than 10% of the annual rainfall over that region. In contrast, across the Sahel and desert border, rainfall totals increase by 15–25 mm/yr which is 5–15% in parts of southern Mauritania, central Mali, and central Chad. Mechanisms for these rainfall changes follow in the section below on surface fluxes and the hydrologic cycle.

5. Temperature Profile

[17] Given the deep vertical transport of mineral aerosols, it is possible that changes in the atmospheric profile of temperature, humidity, and circulation patterns may occur due to the radiative forcing of dust. Therefore, work is completed in examining changes in temperature, specific humidity, zonal/meridional wind speeds, and the moist static energy profile as these atmospheric variables help dictate the evolution of the West African monsoon [*Eltahir and Gong*, 1996; *Gong and Eltahir*, 1996; *Cook*, 1999].

[18] Shown in Figure 8 is the mean JJAS vertical profile of temperature difference between DCONT and CONT simulations zonally averaged from 10°W to 10°E. Clearly seen in the figure is cooling that extends vertically to 700 mb. With a maximum dust burden from 15°N to 20°N, it is expected that this region would experience the most cooling (on the order of 0.5°C–1.0°C). The cooling decreases vertically with decreasing aerosol concentrations. Conversely, around the SAL, there is slight warming from the absorption aloft between 600 and 700 mb. With cooling of the lower atmosphere and warming aloft, mineral aerosols stabilize the atmospheric temperature profile. These results resemble those of other studies that examine changes in the vertical profile of temperature due to dust emissions. For example, *Konare et al.* [2008] find cooling up to 500 mb with a similar slight warming signal from 600 to 700 mb. However, no significant response in wind or circulation patterns is observed.

[19] Figure 8 examines the summertime changes in the vertical distribution of temperature and humidity and the resulting moist static energy profile. As expected, the decrease in temperature leads to a slight decrease in moist static energy from 10°N to 15°N. Across this area, a decrease in moist static energy over a well-mixed region should result in a decrease in rainfall [*Emanuel*, 1995]. As seen in Figure 7, a decrease in rainfall does occur but the magnitude is small, which is consistent with only slight reductions in moist static energy values (0.1–0.2 kJ/kg).

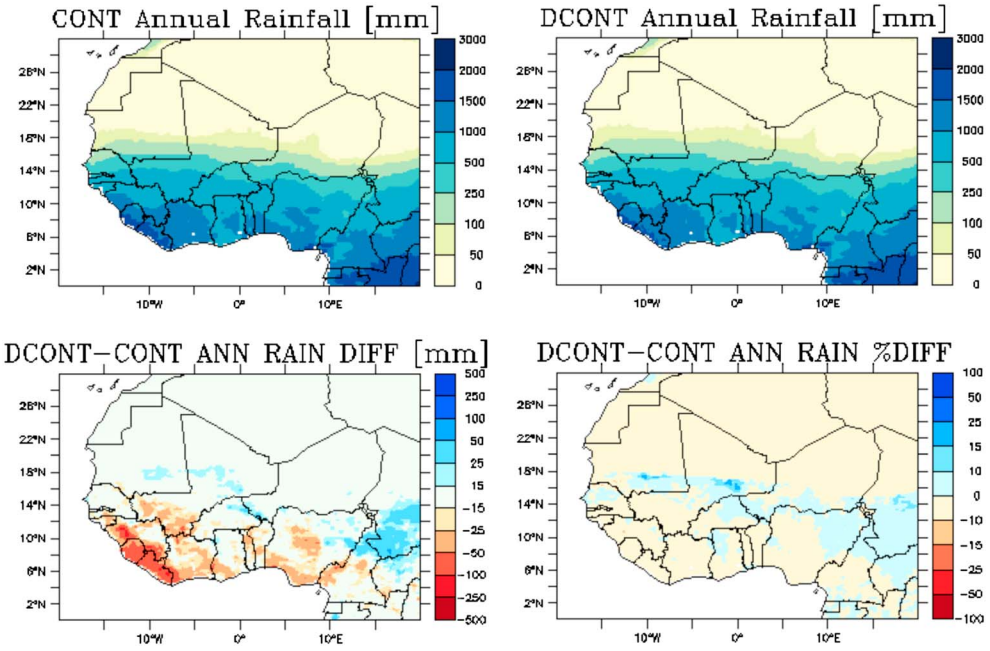

Figure 7. Same as Figure 6 but for annual rainfall (mm/yr). Also plotted is percent difference in annual rainfall between DCONT and CONT. Note that annual rainfall under 100 mm is masked from difference plots.

However, an increase in moist static energy (surface to 700 mb) is observed from 17°N to 25°N despite cooling over this region. Given the equation for moist static energy

$$\mathrm{MSE} = C_p{*}T + L_v{*}w + g{*}z \tag{1}$$

where C_p is the specific heat of air at constant pressure, T temperature, L_v the latent heat of vaporization, w the mixing ratio, g gravity, and z is the elevation above sea level, it can be deduced that if temperatures decrease, an increase in moist static energy can only occur if the mixing ratio (humidity) over the region increases. This intensification is confirmed in Figure 8 where specific humidity values increase 0.2–0.5 g/kg from 15°N to 25°N. The increase in humidity more than compensates for the decrease in temperature and slight increases in moist static energy occur. The increase in humidity from the surface to 800 mb can be attributed to a weakening of the vertical motion or mixing in that layer caused by dust. Essentially, there appears to be a redistribution of moisture in the DCONT simulation as the midatmosphere becomes drier while the surface becomes more humid. The vertical redistribution of humidity is a result of decreased mixing from a shallower boundary layer, which will be discussed later in the next section. With smaller moist static energy (MSE) values from 10°N to 15°N and larger values from 17°N to 25°N, little change

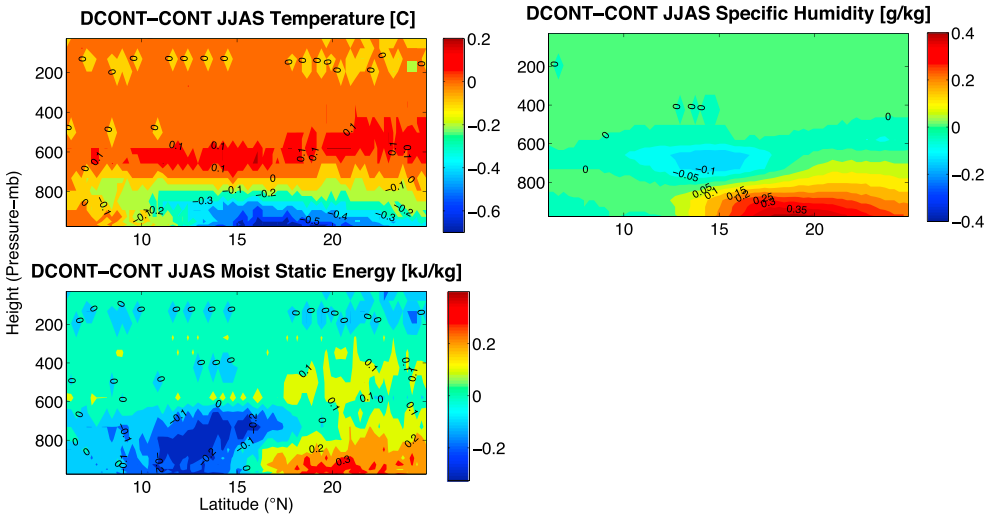

Figure 8. JJAS vertical profiles of DCONT-CONT differences from 6°N to 25°N, zonally averaged from 10°W to 10°W for temperature (°C), specific humidity (g/kg), and moist static energy (kJ/kg).

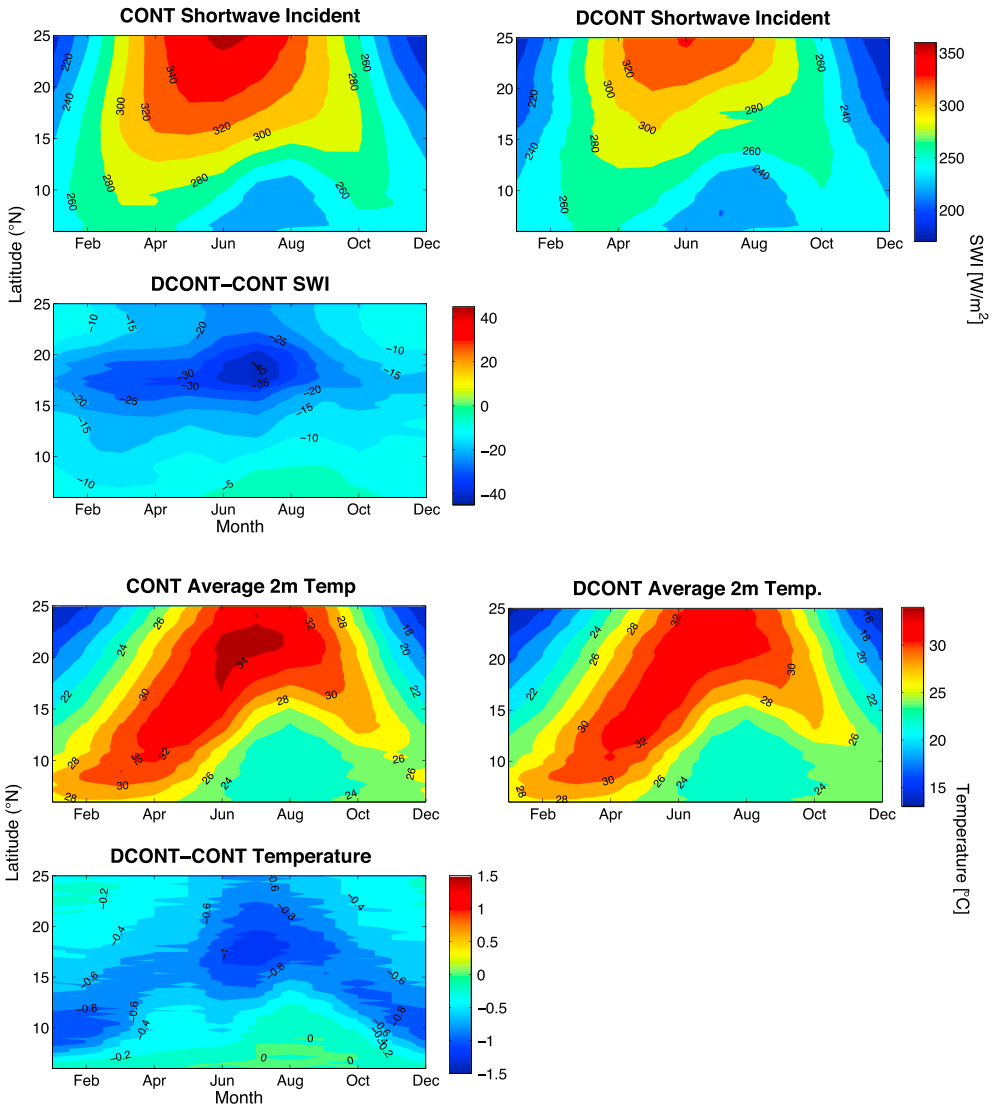

Figure 9. Zonally averaged, (10°W–10°E), monthly average net shortwave radiation (W/m^2) and 2 m temperature (°C) in DCONT and CONT simulations from 6°N to 25°N. Also shown is difference between DCONT and CONT highlighting the effects of dust emissions.

to the moist static energy gradient occurs across the Sahel-Sahara border region. Over this area, changes in the MSE gradient dictate the progression of the monsoon and consequently rainfall. A strengthening in the MSE gradient would result in the monsoon progressing further northward; however, the relative, simulated magnitude of this change in gradient can explain the lack of significant changes in monsoon placement over the border region. That is, the change in gradient is less than 5% of the background gradient across the Sahel/Sahara. Hence, no large change in the monsoon progression is observed. It is important to note that under different dust loading conditions, the results discussed above would change accordingly.

6. Surface Energy Fluxes and Hydrologic Cycle

6.1. Surface Temperature and Shortwave Radiation

[20] Next, work is completed in examining the effects of mineral aerosols on monthly, zonally averaged surface fluxes over West Africa. The largest impact on the surface climatology of West Africa is observed in the shortwave incident radiation (Figure 9). The reduction of net shortwave at the surface ranges from 20 to 40 W/m^2 and strongly follows the spatial and temporal distributions of dust loading shown in Figure 2. More specifically, maximum radiative forcings are found along a swath from 15°N to 20°N with the peak extending from May to August. However, an approximate dust radiative forcing of –10 W/m^2 still reaches to the Gulf of Guinea during the dry months of DJF, when dust events are able to advance southward.

[21] With reductions in net shortwave, net surface cooling is experienced across the entire domain (Figure 9). As expected, maximum cooling (of 1°C for mean daily 2 m temperatures) occurs over the same region during the summertime when dust loading and its radiative forcing are maximized across 15°N–20°N. Surface temperature coolings coincide with the onset of the monsoon, which essentially eliminates the suspension and emissions of dust particles

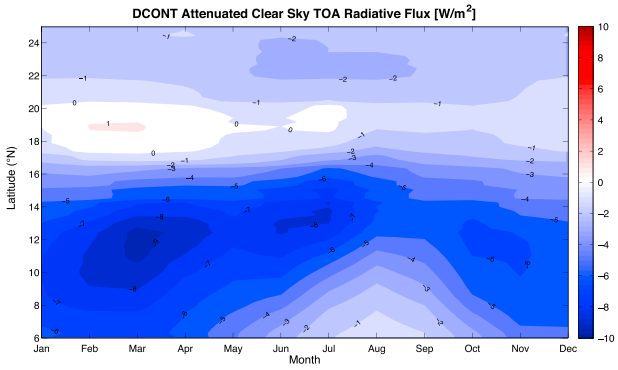

Figure 10. Same as Figure 9 but for DCONT's daily mean clear sky top of atmosphere dust shortwave radiative forcing (W/m^2).

over a region. However, the spatial and temporal signatures in cooling do not completely coincide with AOD or the surface net shortwave dust radiative forcing. For example, a reduction of 0.5°C–1.0°C in mean daily temperature occurs from 8°N to 15°N during the winter and spring seasons even though surface shortwave downward radiation is only attenuated by 10 W/m^2. Over this region, the surface net shortwave as well as the TOA net dust radiative forcing is negative; hence, cooling is more pronounced even with a smaller net shortwave radiative forcing at the surface, assuming no significant change in the surface upward shortwave across the desert region. We expect little change in the upward due to the lack of changes in soil moisture or vegetative patterns across this region—the two main drivers for surface albedo and subsequent changes in upward shortwave. This result can be explained by the scattering properties of dust particles over dark vegetated regions; that is, when the surface is darker, scattering aerosols are more effective at reducing the amount of sunlight absorbed by the surface. Even though the surface radiative forcing is not as substantial as that over the Sahara, the TOA radiative forcing is actually larger from 8°N to 12°N than from 15°N to 20°N (Figure 10). In fact, it can be seen that from 6°N to 15°N, the cooling signature of Figure 9 follows the negative TOA radiative forcing. Farther north, the TOA forcing is negligible due to the desert surface being quite bright already; therefore, the surface upward shortwave radiation forcing is small. These results are consistent with higher SSA values simulated over that region. Essentially, the resulting dust loading effects on radiation and temperature are more sensitive over these darker regions since the increase in shortwave radiation upward over these areas are larger than over desert regions further north.

6.2. Monthly Rainfall and Moist Static Energy

[22] Examining monthly changes in the daily rainfall rate (Figure 11) confirms the results presented in Figure 7—rainfall patterns over the region are left largely unchanged by dust emissions. A slight decrease in rainfall occurs along the monsoon onset and retreat, but these values are on the order of <5% of the daily rainfall values (Figure 11). As alluded to prior, across this land-ocean border, which is a well-mixed region, a decrease in net radiation would result in a decrease in moist static energy and subsequently rainfall [*Polcher*, 1995; *Emanuel*, 1995]. Figure 12 shows slight decreases in the moist static energy from November to April over this area. Consequently, the onset (recession) of the monsoon is delayed (accelerated) and rainfall during the spring (fall) decreases along the monsoon front from 6°N to 12°N. These results are somewhat different than *Konare et al.* [2008] and *Solmon et al.* [2008], which report a small increase in rainfall across the Gulf of Guinea.

[23] Across the desert border region, we observe either no change or a slight increase in rainfall in some regions due to an increase in convective efficiency. These results are quite different than *Konare et al.* [2008] which report decreases in rainfall over the Sahel yet similar to *Solmon et al.* [2008], which find slight increases across Mauritania, Mali, and Niger in rainfall. In *Konare et al.*'s [2008] study, the simulations indicated a decrease in the moist static energy gradient and a weakening in the monsoon energy pump—it is well known that the magnitude and gradient of MSE plays a large

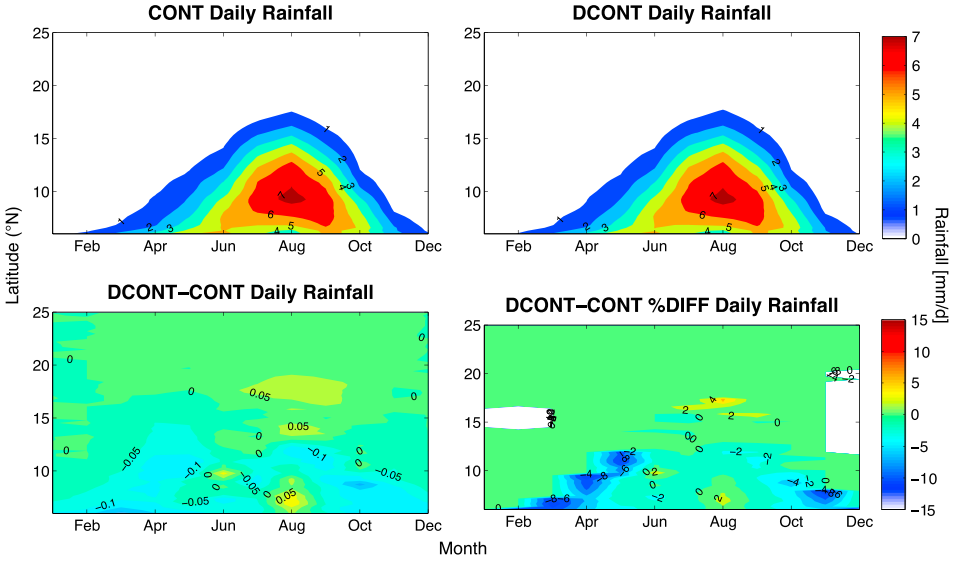

Figure 11. Same as Figure 9 but for daily rainfall rates (mm/d).

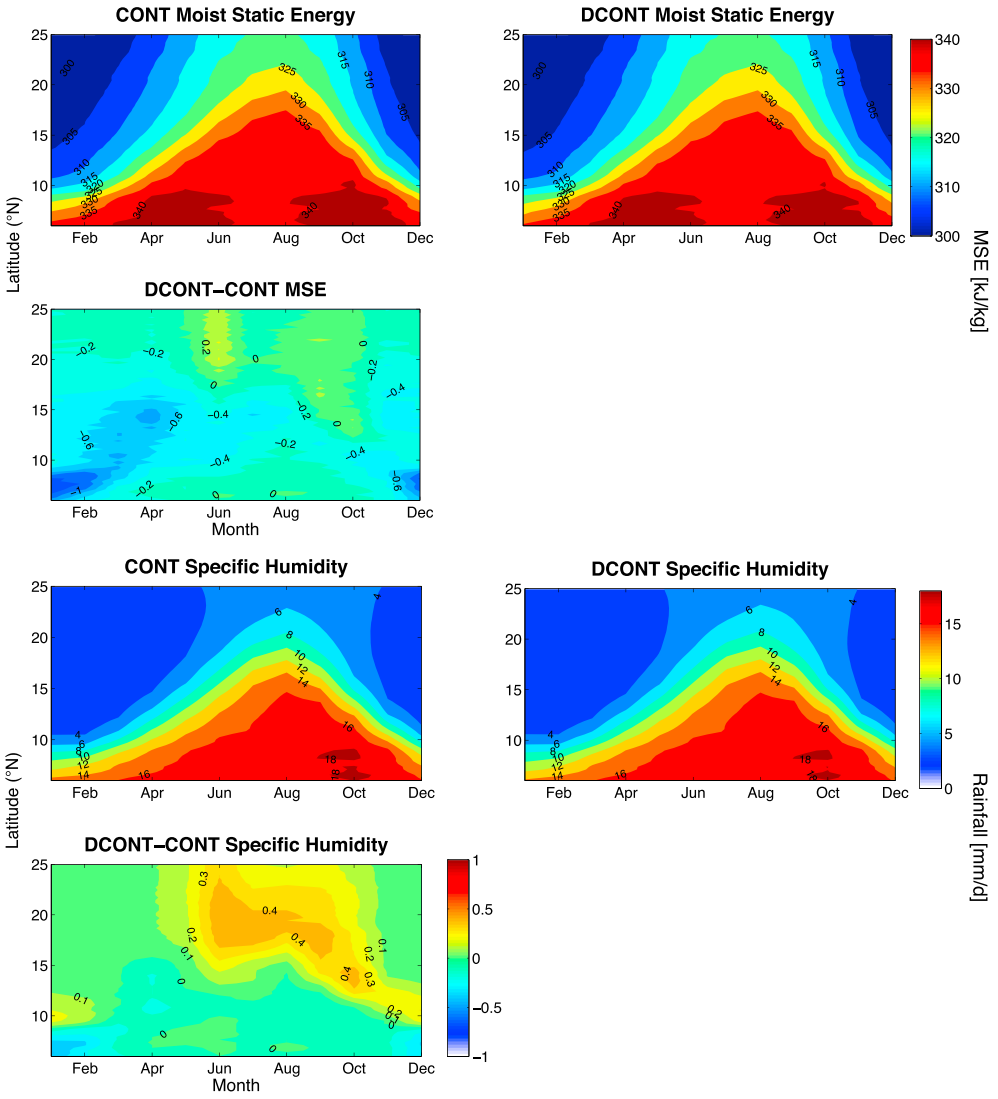

Figure 12. Same as Figure 9 but for moist static energy (kJ/kg) and surface specific humidity (g/kg).

role in the evolution of the West African monsoon and convection in general [*Eltahir and Gong*, 1996; *Fontaine et al.*, 2002]. Here our simulations find that the surface moist static energy (MSE) gradient is left largely unaltered with only slight increases caused by dust emissions across the Sahel (Figure 12). As mentioned when discussing changes in the atmospheric temperature profile, the lack of change or slight increase in surface MSE can be explained by an increase in humidity that occurs across the Sahel and southern Sahara from June to October (Figure 12). Over the desert border, mean daily 10 m specific humidity values increase from 0.25 to 0.5 g/kg. With cooler temperatures and more humid conditions, the relative humidity over the region increases by 5 to 10% and the MSE increases in the boundary layer. As a result, convective efficiency is enhanced and rainfall increases [*Eltahir*, 1998]. Nevertheless, the slight increase in humidity can be attributed to moisture redistribution over this region due to a shallower boundary layer. With a shallower boundary layer, less mixing occurs aloft and moisture is confined to the lower atmosphere and not advected out of the region via the AEJ. Therefore, the cooling of temperature is counteracted by the increase in moisture where surface MSE values remain largely similar and rainfall patterns nearly identical. Again, it is important to note that these changes are quite small, and hence, the rainfall respons is as such.

6.3. Surface Heat Fluxes and Boundary Layer Height

[24] With the reduction in shortwave incident, it is expected that the entire surface energy balance will respond to the mineral aerosol radiative forcing. Decreases in the net radiation are experienced across the entire domain particularly across the Sahel region from April to August where values are lower by 10–15 W/m^2. The reduction is consistent with the shortwave attenuation as well as a decrease in net longwave radiation. With very slight changes in the downward longwave radiation found, it can be inferred that the change in net longwave is a result of less upward longwave caused by surface cooling. Nevertheless, the resulting change in net radiation must be balanced by the latent and sensible heat fluxes at the surface. Overall, little change in the latent heat flux is found across the region (2–4W/m^2)

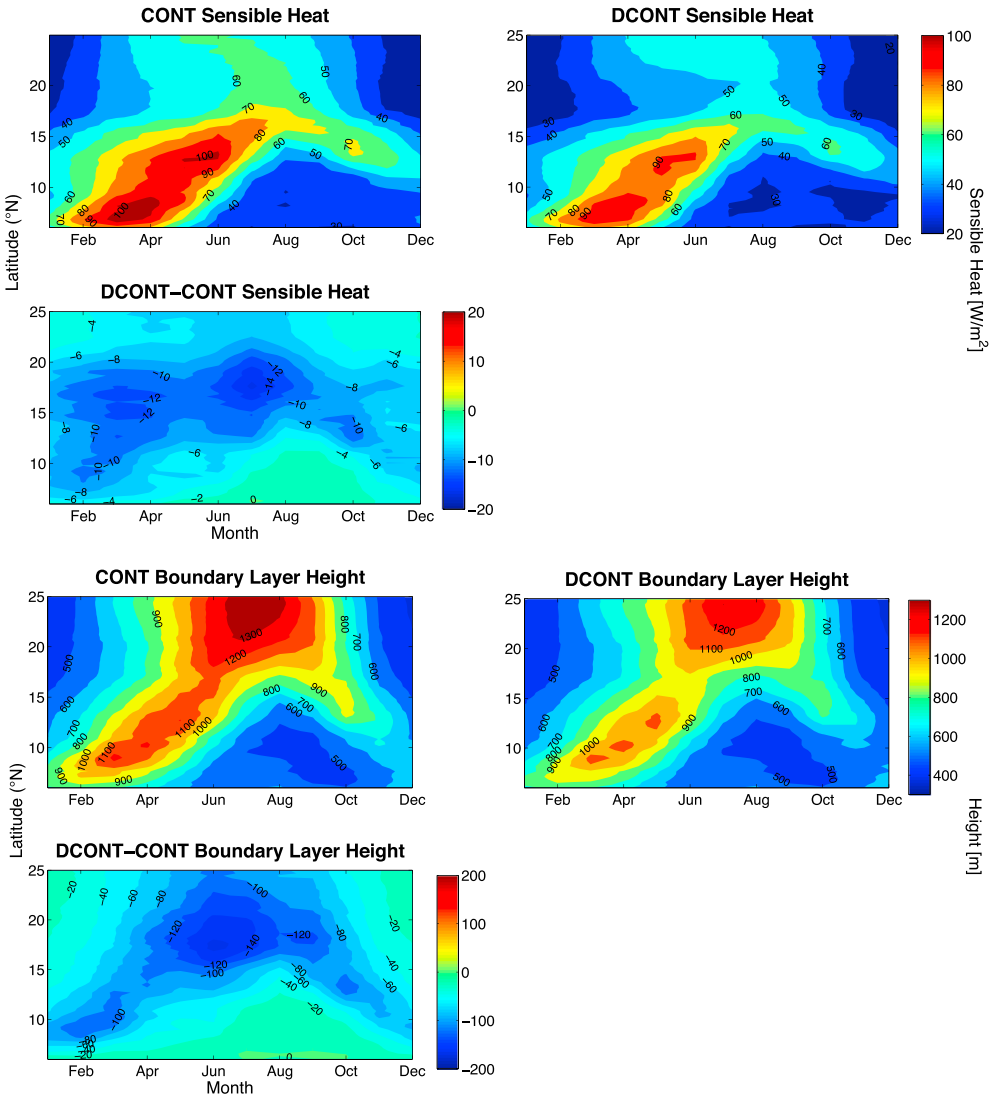

Figure 13. Same as Figure 9 but for the sensible heat flux (W/^{2}) and boundary layer height (m).

and is consistent with the lack of rainfall changes and dry soil moisture conditions. However, Figure 13 reveals that the reduction in sensible heat flux largely compensates for changes in the net radiation. For example, a 10–15 W/m^2 reduction in net radiation from during the spring and summer is met with an identical decrease in the sensible heat flux. The difference in net radiation's temporal and spatial signatures nearly matches that of the sensible heat (not shown). These results are consistent with the aforementioned cooling of surface temperature.

[25] Lastly, important for changes in convective rainfall, the effects of dust on planetary boundary layer (PBL) height is examined. Given the reduction in surface temperature and sensible heat, a decrease in mechanical mixing should limit the growth of the boundary layer, particularly in regions with strong responses to mineral aerosols. This effect is confirmed in Figure 13. Over the Sahel region, average daily boundary layer heights decrease by approximately 100–150 m which is a nearly 15% decrease in height. These results follow the same temporal and spatial signatures of the sensible heat flux reduction and 2 m temperature cooling. However, when examining a diurnally strong atmospheric feature such as boundary layer height, the use of daily averaged, monthly values smooth the signal. The three-hourly model output data reveal that dust emissions can reduce the boundary layer height by nearly 1 to 2 km during its peak in late afternoon (see Figure 14). With mineral aerosols reducing the incident shortwave radiation, it is expected that the response to the boundary layer growth and temperature will respond diurnally as well, similar to the incoming shortwave radiation diurnal cycle. These results have large implications on the moisture distribution in the atmosphere. Given a significantly shallower boundary layer, moisture that normally would mix upward and then advect out of the region via the AEJ is now constrained closer to the surface in a more stagnant layer. The mechanism is shown in Figure 15 which plots the northward evolution of the change in boundary layer height and surface humidity as a result of mineral aerosols (DCONT-CONT). Clearly evident in the figure is the northward decrease in boundary layer height while at the same

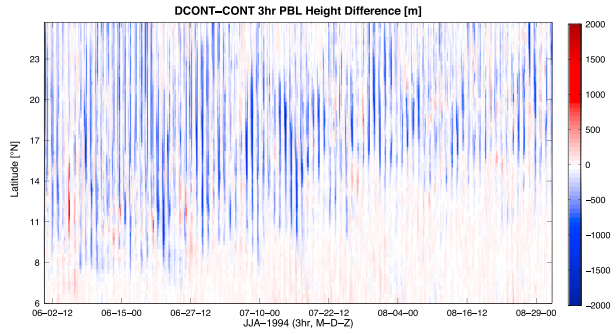

Figure 14. Difference between DCONT and CONT planetary boundary layer height (m) every 3 h for the months of June–August for the year 1994. Note these results are averaged from 15°N to 20°N and 10°W to 10°E.

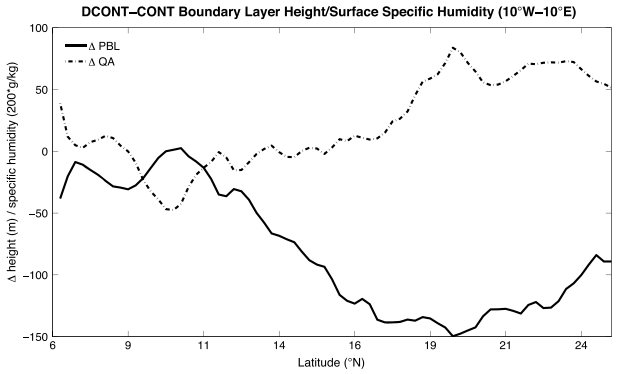

Figure 15. Change (DCONT-CONT) in JJAS average boundary layer height (solid line, in meters) and specific humidity (dashed line, in g/kg) from 6°N to 25°N, zonally averaged from 10°W to 10°E. Note that the specific humidity is scaled by a factor of 200 to show symmetry with boundary layer height differences.

time a northward increase in surface humidity occurs. For example, maximum increases in surface moisture occur at the same location of maximum boundary layer height decay (approximately 19°N) whereas from 6°N to 12°N, little change in surface moisture or boundary layer height occurs due to mineral aerosols. This result explains the increased surface and low-level atmospheric moisture and hence the lack of change in moist static energy across the desert border region.

7. Summary and Conclusions

[26] This work highlights the effects of dust emissions on the climate of West Africa. First, it is found that RegCM3-IBIS does well in simulating the mineral aerosol climatology over the region. That is, the model is able to reproduce successfully the temporal trends and spatial patterns of dust suspension over the Sahel and Sahara. As a result, dust emissions overall cool not only the surface of West Africa but also aloft to 700 mb. A significant portion of this cooling is a result of scattering and therefore attenuation of shortwave incident radiation on the order of 25–40 W/m^2. However, it is important to note that there is still significant absorption aloft caused by dust as well.

[27] Overall, slight changes are found in rainfall patterns which are consistent with a lack of any significant change in moist static energy or its gradient across West Africa. However, two distinct regions exist in the effects of mineral aerosols on West African rainfall. From the coast to 15°N, very small reductions in the moist static energy result in a small reduction in rainfall, whereas across the Sahel-Sahara border, the changes in the surface moist static energy gradient are negligible compared to the background gradient and rainfall remains largely unchanged; slight increases across Mauritania, Mali, and Niger are a result of increased convective efficiency (i.e., higher relative humidity and MSE in the boundary layer). Across the Sahel-Sahara region, cooling by mineral aerosols is compensated by moistening found over the region during the summertime months; as a result, no sizable change in moist static energy occurs. Lastly, no change is found in the interannual variability of rainfall across the region; that is, there is no significant correlation between dusty and wet/dry years across the Sahel observed. Table 2 summarizes the changes in daily average summertime surface climate variables across the dust belt of 10°W–10°E and 15°N–20°N as a result of dust emissions.

[28] The increase in humidity across the desert border region can be explained by a decrease in vertical mixing caused by stratification (cooling near surface, warming aloft) of the atmosphere by suspended dust. Essentially, mineral aerosols cause a redistribution of moisture closer to the surface due to a decrease in boundary layer height. As a result, areas that cool because of dust suspension also become more humid, due to a shallower boundary layer. Figure 16 presents a schematic highlighting the mechanisms behind these processes across the two regions.

[29] Many opportunities still exist in examining the effects of mineral aerosols over West Africa. Namely, as alluded to prior with boundary layer depths, extensive analysis at the diurnal timescale should be completed and will most likely yield larger effects caused by dust. That is, the daily averaging computed above most likely mutes the dust forcing signal on humidity and circulation patterns. On a finer physical scale, further research should explore the regional modeling of the indirect effects of mineral aerosols such as those on cloud microphysics while still including its direct, radiative effects; many studies have offered contrasting views of the cloud-mineral aerosol interaction with some finding that dust as a cloud condensation nuclei decreases rainfall [e.g., *Rosenfeld et al.*, 2001; *Hui et al.*, 2008; *Kluser and Holzer-Popp*, 2010] while others postulate that dust

Table 2. Summary of JJA Average Daily Shortwave Incident Radiation (SWI, W/m^2), Temperature (TA, °C), Boundary Layer Height (PBL, m), Specific Humidity (QA, g/kg), Rainfall (PRE, mm/mon), Latent Heat (LH, W/m^2), and Sensible Heat (SH, W/m^2), in CONT and DCONT simulations for the period of 1973–2002 averaged over 10°W–10°E and 15°N–20°N[a]

	SWI	TA	PBL	QA	PRE	LH	SH
CONT	319	31.8	1048	10.2	23.7	20.4	70.4
DCONT	288	30.8	919	10.6	24.7	20.5	57.9
DCONT-CONT	–31	–1.0	–129	0.4	1.0	0.1	–12.5

[a]Also shown is the difference between the two simulations.

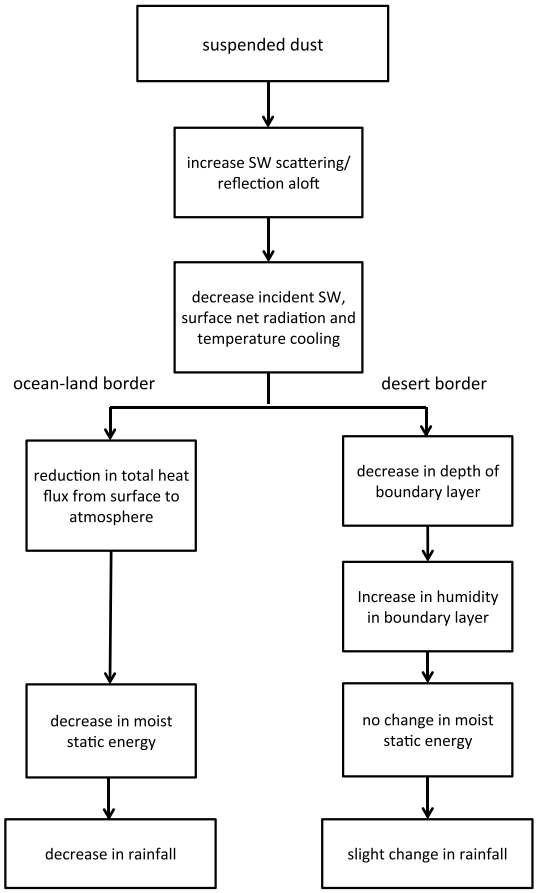

Figure 16. Schematic highlighting the effects of dust on humidity, temperature, moist static energy, and ultimately rainfall over two distinct regions of West Africa: the land-ocean border (6°N–14°N) and the desert border region (15°N–20°N).

increases cold-rain precipitation as ice condensation nuclei [e.g., *DeMott et al.*, 2003; *Jenkins et al.*, 2008]. Likewise, as alluded prior, the effects of the full suite of West African aerosols including anthropogenic (biomass burning) and natural (lightning strikes) carbonaceous aerosols on the region's climate, combined with dust, should be examined on the climate scale of regional modeling.

[30] Given that most regional models use prescribed SSTs, inherently these models are accounting for changes in surface temperature caused by dust emissions. Further work should look to quantify the temperature change caused by dust on sea surface temperatures and experiments performed with these adjusted "nondust" SSTs. Given the results above and those of *Malavelle et al.* [2011], it is possible that the total radiative effects of these aerosols could greatly affect the West African Monsoon. Moreover, as observed in *Wilcox et al.* [2010], Saharan dust outbreaks have been linked to a northward shift in the Atlantic Intertropical Convergence Zone. Therefore, the effects of suspended dust on surface temperatures over the ocean should be more carefully examined. The same bias (in the opposite direction) in boundary conditions can also be argued as ERA-40 values account for dust which reduces the boundary temperature profile by 1°K in some situations. Lastly, the interaction between vegetation dynamics and dust emissions, which may be significant in determining the mineral aerosol forcing on regional climates, particularly that of West Africa, should be explored via a model like RegCM3-IBIS.

References

Abdou, W. A., D. A. Diner, J. V. Martonchik, C. J. Bruegge, R. A. Kahn, B. J. Gaitley, K. A. Crean, L. A. Remer, and B. Holben (2005), Comparison of coincident Multiangle Imaging Spectroradiometer and Moderate Resolution Imaging Spectroradiometer aerosol optical depths over land and ocean scenes containing Aerosol Robotic Network sites, *J. Geophys. Res.*, *110*, D10S07, doi:10.1029/2004JD004693.

Brooks, N., and M. Legrand (2000), *Dust Variability Over Northern Africa and Rainfall in the Sahel*, chap. 1, pp. 1–25, Linking Climate Change to Land Suface Change, Springer, Neth.

Carlson, T., and J. M. Prospero (1972), The large-scale movement of Saharan air outbreaks over the northern equatorial Atlantic, *J. Appl. Meteorol.*, *11*, 283–297.

Cook, K. H. (1999), Generation of the African easterly jet and its role in determining West African precipitation, *J. Clim.*, *12*, 1165–1184.

Cooke, W. F., C. Liousse, H. Cachier, and J. Feichter (1999), Construction of a 1 degrees by 1 degrees fossil fuel emission dataset for carbonaceous aerosol and implementation and radiative impact in ECHAM4 model, *J. Geophys. Res.*, *104*, 22,137–22,162.

DeMott, P. J., K. Sassen, M. R. Poellot, D. Baumgardner, D. C. Rogers, S. D. Brooks, A. J. Prenni, and S. M. Kreidenweis (2003), African dust aerosols as atmospheric ice nuclei, *Geophys. Res. Lett.*, *30*(14), 1732, doi:10.1029/2003GL017410.

Eltahir, E. A. (1998), A soil moisture–rainfall feedback mechanism. 1. Theory and observations, *Water Resour. Res.*, *34*(4), 765–776.

Eltahir, E. A. B., and C. Gong (1996), Wet and dry years in West Africa, *J. Clim.*, *9*, 1030–1042.

Emanuel, K. A. (1995), On thermally direct circulations in moist atmospheres, *J. Atmos. Sci.*, *48*, 2313–2335.

Foley, J., I. Prentice, N. Ramankutty, S. Levis, D. Pollard, S. Sitch, and A. Haxeltine (1996), An integrated biosphere model of land surface processes, terrestrial carbon balance, and vegetation dynamics, *Global Biogeochem. Cycles*, *10*(4), 603–628.

Fontaine, B., N. Philippon, S. Trzaska, and P. Roucou (2002), Spring to summer changes in the West African monsoon through NCEP/NCAR reanalyses (1968–1998), *J. Geophys. Res.*, *107*(D14), 4186–4194, doi:10.1029/2001JD000834.

Gong, C., and E. A. B. Eltahir (1996), Source of moisture for rainfall in West Africa, *Water Resour. Res.*, *32*(10), 3115–3121.

Grell, G. A., J. Dudhia, and D. Stauffer (1994), A description of the fifth-generation Penn State/NCAR Mesoscale Model (MM5), *Tech. Note TN-398+IA*, Natl. Cent. for Atmos. Res., Boulder, Colo.

Haywood, J., P. Francis, S. Osborne, M. Glew, N. Loeb, E. Highwood, D. Tanre, G. Myhre, P. Formenti, and E. Hirst (2003), Radiative properties and direct radiative effect of Saharan dust measured by the C-130 aircraft during SHADE: 1. Solar spectrum, *J. Geophys. Res.*, *108*(D18), 8577, doi:10.1029/2002JD002687.

Haywood, J., J. Pelon, P. Formenti, N. Bharmal, N. Brooks, F. Capes, P. Chazette, D. Tanre, and P. Tulet (2008), Overview of dust and biomass-burning experiment and African monsoon multidisciplinary analysis special observing period, *J. Geophys. Res.*, *113*, D00C17, doi:10.1029/2008JD010077.

Hsu, N., S. C. Tsay, M. D. King, and J. Herman (2004), Aerosol properties over bright-reflecting source regions, *IEEE Trans. Geosci. Remote Sens.*, *42*, 557–569.

Hui, W., B. Cook, S. Ravi, J. Fuentes, and P. D'Odorico (2008), Dust-rainfall feedbacks in the West African Sahel, *Water Resour. Res.*, *44*, W05202, doi:10.1029/2008WR006885.

Jenkins, G., A. Pratt, and A. Heymsfield (2008), Possible linkages between Saharan dust and tropical cyclone rain band invigoration in the eastern Atlantic during NAMMA-06, *Geophys. Res. Lett.*, *35*, L08815, doi:10.1029/2008GL034072.

Junker, C., and C. Liousse (2008), A global emission inventory of carbonaceous aerosol from historic records of fossil fuel and biofuel consumption for the period 1860–1997, *Atmos. Chem. Phys.*, *8*(5), 1195–1207.

Kaufman, Y. J., D. Tanre, O. Dubovik, A. Karnieli, and L. A. Remer (2001), Absorption of sunlight by dust as inferred from satellite and ground-based remote sensing, *Geophys. Res. Lett.*, *28*, 1479–1482.

Kluser, L., and T. Holzer-Popp (2010), Relationships between mineral dust and cloud properties in the West African Sahel, *Atmos. Chem. Phys.*, *10*(14), 6901–6915.

Konare, A., A. S. Zakey, F. Solmon, F. Giorgi, S. Rauscher, S. Ibrah, and X. Bi (2008), A regional climate modeling study of the effect of desert dust on the West African monsoon, *J. Geophys. Res.*, *113*, D12206, doi:10.1029/2007JD009322.

Lau, K. M., K. Kim, Y. Sud, and J. Walker (2009), A GCM study of the response of the atmospheric water cycle of West Africa and the Atlantic to Saharan dust radiative forcing, *Annu. Geophys.*, *27*(19), 4023–4037.

Liao, H., and J. Seinfeld (1998), Radiative forcing by mineral dust aerosol: Sensitivity to key variables, *J. Geophys. Res.*, *103*(31), 637–646.

Liousse, C., J. E. Penner, C. Chuang, J. Walton, H. Eddleman, and H. Cachier (1996), A global three-dimensional model study of carbonaceous aerosols, *J. Geophys. Res.*, *101*, 19,411–19,432.

Mahowald, N., K. Kohfeld, M. Hansoon, Y. J. Balkanski, P. Harrison, I. Prentice, M. Schulz, and H. Rodhe (1999), Dust sources and deposition during the last glacial maximum and current climate: A comparison of model results with paleodata from ice cores and marine sediments, *J. Geophys. Res.*, *104*, 15,895–15,916.

Malavelle, F., V. Pont, M. Mallet, F. Solmon, B. Johnson, J. Leon, and C. Liousse (2011), Simulation of aerosol radiative effects over West Africa during DABEX and AMMA SOP-0, *J. Geophys. Res.*, *116*, D08205, doi:10.1029/2010JD014829.

Marcella, M. P., and E. A. B. Eltahir (2010), Effects of mineral aerosols on the summertime climate of southwest Asia: Incorporating subgrid variability in a dust emission scheme, *J. Geophys. Res.*, *115*, D18203, doi:10.1029/2010JD014036.

Martonchik, J. V., D. J. Diner, R. A. Kahn, T. P. Ackerman, M. M. Verstraete, B. Pinty, and H. R. Gordon (1998), Techniques for the retrieval of aerosol properties over land and ocean using multiangle imaging, *IEEE Trans. Geosci. Remote Sens.*, *35*, 1212–1227.

Miller, R., and I. Tegen (1998), Climate response to soil dust aerosols, *J. Clim.*, *11*, 3247–3267.

Miller, R. L., J. Perlwitz, and I. Tegen (2004), Feedback upon dust emission by radiative forcing through the planetary boundary layer, *J. Geophys. Res.*, *109*, D24209, doi:10.1029/2004JD004912.

Milton, S., G. Greed, M. Brooks, J. Haywood, B. Johnson, R. Allan, A. Slingo, and W. Grey (2008), Modeled and observed atmospheric radiation balance during the West African dry season: Role of mineral dust, biomass burning aerosol, and surface albedo, *J. Geophys. Res.*, *113*, D00C02, doi:10.1029/2007JD009741.

Pal, J., et al. (2007), Regional climate modeling for the developing world: The ICTP RegCNET and RegCM, *Bull. Am. Meteorol. Soc.*, *88*(9), 1395–1409.

Perkey, D. J., and C. W. Kreitzberg (1976), A time-dependent lateral boundary scheme for limited-area primitive equation models, *Mon. Weather Rev.*, *104*, 744–755.

Polcher, J. (1995), Sensitivity of tropical convection to land surface processes, *J. Atmos. Sci.*, *52*(17), 3143–3163.

Prospero, J. M., P. Ginoux, O. Torres, E. Nicholson, and T. E. Gill (2002), Environmental characterization of global sources of atmospheric soil dust identified with the Nimbus 7 total ozone mapping spectrometer (TOMS) absorbing aerosol product, *Rev. Geophys.*, *40*(1), 1002, doi:10.1029/2000RG000095.

Ramankutty, N., and J. Foley (1998), Characterizing patterns of global land use: An analysis of global croplands data, *Global Biogeochem. Cycles*, *12*(4), 667–685, doi:10.1029/98GB02512.

Rayner, N., D. Parker, E. Horton, C. Folland, L. Alexander, D. Rowell, E. Kent, and A. Kaplan (2006), UKMO - GISST/MOHMATN4/MOHSST6 - Global Ice Coverage and SST (1856-2006).

Rosenfeld, D., Y. Rudich, and R. Lahav (2001), Desert dust suppressing precipitation: A possible desertification feedback loop, *Proc. Nat. Acad. Sci. U.S.A.*, *98*, 5975–5980.

Sokolik, I. N., D. M. Winker, G. Bergametti, D. A. Gillette, G. Carmichael, Y. J. Kaufman, L. Gomes, L. Schuetz, and J. E. Penner (2001), Introduction to special section: Outstanding problems in quantifying the radiative impacts of mineral dust, *J. Geophys. Res.*, *106*, 18,015–18,027.

Solmon, F., F. Giorgi, and C. Liousse (2006), Aerosol modelling for regional climate studies: Application to anthropogenic particles and evaluation over a European/African domain, *Tellus B*, *58*(1), 51–72.

Solmon, F., M. Mallet, N. Elguindi, F. Giorgi, A. S. Zakey, and A. Konare (2008), Dust aerosol impact on regional precipitation over western Africa, mechanisms and sensitivity to absorption properties, *Geophys. Res. Lett.*, *35*, L24705, doi:10.1029/2008GL035900.

Tegen, I., A. A. Lacis, and I. Fung (1996), The influence of climate forcing of mineral aerosols from disturbed soils, *Nature*, *380*, 419–422.

Uppala, S., et al. (2005), The ERA-40 Re-analysis, *Q. J. R. Meteorol. Soc.*, *131*(612), 2961–3012.

Wilcox, E. M., W. K. M. Lau, and K. Kim (2010), A northward shift of the North Atlantic Ocean Intertropical Convergence Zone in response to summertime Saharan dust outbreaks, *Geophys. Res. Lett.*, *37*, L04804, doi:10.1029/2009GL041774.

Winter, J. M., J. Pal, and E. A. B. Eltahir (2009), Coupling of integrated biosphere simulator to regional climate model version 3, *J. Clim.*, *22*, 2743–2757.

Woodward, S. (2001), Modeling the atmospheric life cycle and radiative impact of mineral dust in the Hadley Centre climate model, *J. Geophys. Res.*, *106*, 18,155–18,166.

Yoshioka, M. N., N. Mahowald, A. Conley, W. Collins, W. Fillmore, C. Zender, and D. Coleman (2007), Impact of dust radiative forcing on Sahel precipitation: Relative importance of dust compared to sea surface temperature variations, vegetation changes, and greenhouse gas warming, *J. Clim.*, *20*, 1445–1467.

Zakey, A., F. Solmon, and F. Giorgi (2006), Implementation and testing of a desert dust module in a regional climate model, *Atmos. Chem. Phys.*, *6*, 4687–4704.

Zhang, D. F., A. S. Zakey, X. J. Gao, F. Giorgi, and F. Solmon (2009), Simulation of dust aerosol and its regional feedbacks over East Asia using a regional climate model, *Atmos. Chem. Phys.*, *9*, 1095–1110.